Volume 1 | Number 1 | Jan 2013 | Pages 1–100

ChemComm

Chemical Communications
www.rsc.org/chemcomm

ROYAL SOCIETY OF CHEMISTRY

This is an *Accepted Manuscript*, which has been through the Royal Society of Chemistry peer review process and has been accepted for publication.

Accepted Manuscripts are published online shortly after acceptance, before technical editing, formatting and proof reading. Using this free service, authors can make their results available to the community, in citable form, before we publish the edited article. We will replace this *Accepted Manuscript* with the edited and formatted *Advance Article* as soon as it is available.

You can find more information about *Accepted Manuscripts* in the **Information for Authors**.

Please note that technical editing may introduce minor changes to the text and/or graphics, which may alter content. The journal's standard **Terms & Conditions** and the **Ethical guidelines** still apply. In no event shall the Royal Society of Chemistry be held responsible for any errors or omissions in this *Accepted Manuscript* or any consequences arising from the use of any information it contains.

ROYAL SOCIETY OF CHEMISTRY

www.rsc.org/chemcomm

Journal Name

COMMUNICATION

Mechanistic insight into the hydroxylation of alkanes by a nonheme iron(V)-oxo complex†

Eunji Kwon,[a] Kyung-Bin Cho,[a] Seungwoo Hong[a] and Wonwoo Nam[a]*

**Hydroxylation of alkanes by a mononuclear nonheme iron(V)-oxo complex, $[Fe(V)(O)(TAML)]^-$, is initiated by a rate-determining hydrogen atom (H-atom) abstraction, followed by an oxygen non-rebound process. Evidence for the H-atom abstraction/oxygen non-rebound mechanism is obtained experimentally and supported by DFT calculations.**

High-valent iron-oxo intermediates of heme and nonheme ligands are ubiquitous in nature and perform a wide range of important biological and chemical oxidation reactions.[1,2] In cytochrome P450 (CYP 450) and their iron porphyrin models, high-valent iron(IV)-oxo porphyrin π-cation radicals, referred to compound I (Cpd I), are active oxidants in a variety of oxygenation reactions, including alkane hydroxylation.[1,3] The hydroxylation of alkanes by Cpd I in CYP 450 and iron porphyrin models is initiated by a rate-determining hydrogen abstraction step by (Porp$^{\bullet +}$)Fe(IV)O, followed by an oxygen rebound step between the resulting (Porp)Fe(IV)OH and substrate radical species.[4]

High-valent iron(IV)-oxo species have also been trapped in nonheme iron enzymes and successfully synthesized in biomimetic models.[2,5] The nonheme iron(IV)-oxo species have shown reactivities in the activation of C-H bonds of substrates. The C-H bond activation by nonheme iron(IV)-oxo species occurs via a hydrogen atom (H-atom) abstraction mechanism, in which the H-atom abstraction is the rate-determining step (r.d.s.) (Scheme 1A, pathway a).[6] However, different from the heme systems, the C-H bond activation does not occur via the H-atom abstraction/oxygen rebound mechanism. For instance, a substrate:catalyst product ratio closer to 1:2 has been experimentally observed, instead of the 1:1 stoichiometry that is postulated for a rebound reaction.[7] Instead, it has been shown that dissociation of the substrate radical (Scheme 1A, pathway c) is more favourable than the oxygen rebound process (Scheme 1A, pathway b).[7b] The oxygen non-rebound mechanism has also been observed in the reactions of nonheme Mn(IV)-oxo and Cr(IV)-oxo complexes (Scheme 1A).[8]
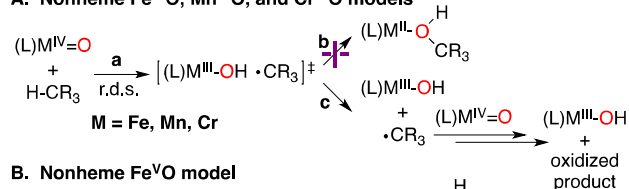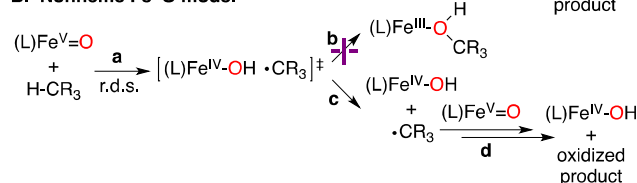
Scheme 1

Nonheme iron(V)-oxo species have been proposed frequently as key intermediates in biological and synthetic oxidation reactions;[9,10] however, there are only a couple of synthetic nonheme iron(V)-oxo complexes reported so far.[11,12] One notable example is an iron(V)-oxo complex bearing tetraamido macrocyclic ligand (TAML), $[Fe(V)(O)(TAML)]^-$.[11] This iron(V)-oxo complex has shown reactivities in C-H bond activation as well as in olefin epoxidation and sulfoxidation.[11,13] Very recently, Sen Gupta reported elegant results on the activation of unactivated C-H bonds by a room temperature stable iron(V)-oxo complex bearing a TAML derivative.[14] However, mechanism of the hydroxylation of alkanes by nonheme iron(V)-oxo species has been less clearly understood (e.g., oxygen rebound versus oxygen non-rebound mechanism; Scheme 1B, pathways b versus c). We therefore performed mechanistic studies on the hydroxylation of alkanes by the iron(V)-oxo complex, $[Fe(V)(O)(TAML)]^-$ (**1**). Herein we report experimental and theoretical evidence suggesting that the alkane hydroxylation by the iron(V)-oxo complex occurs via a H-atom abstraction/oxygen non-rebound mechanism (Scheme 1B).

Commercially available *m*-chloroperoxybenzoic acid (*m*-CPBA, 55%) was purified to 94% based on the ratio of *m*-CPBA and *m*-CBA (*m*-chlorobenzoic acid) in ^{1}H NMR spectrum (see Fig. S2c, ESI†).
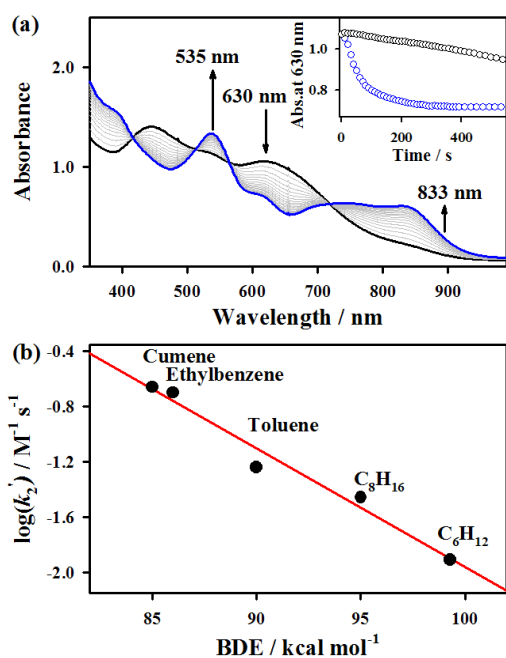
Fig 1. (a) UV-vis spectral changes of **1** (0.25 mM, red line) upon addition of 30 equiv. of ethylbenzene in CH_3CN at 0 °C. Inset shows time course recorded at 630 nm for the natural decay of **1** (black circle) and the reaction of **1** with substrate (blue circle). (b) Plot of log k_2' against the substrates C-H BDE. Second-order rate constants, k_2, were determined and then adjusted for reaction stoichiometry to yield k_2' based on the number of equivalent target C-H bonds of substrates (see data in Fig. S4 and Table S1, ESI†).

$Na(H_2O)_x[Fe(III)(TAML)]$ complex was purchased and purified by recrystallization from iso-propanol/H_2O mixture (further details can be found in ESI†). Previous studies showed that it is possible to generate iron(V)-oxo species **1** at −40 °C in CH_3CN by reacting 3 equiv. of m-CPBA with $[Fe(III)(TAML)]^−$.[11] Following this procedure, we prepared **1** by reacting $[Fe(III)(TAML)]^−$ (0.25 mM) with 3 equiv. of m-CPBA in CH_3CN at both −40 °C and 0 °C (Fig. 1a and Figs. S1 and S2, ESI†) with good yields based on the extinction coefficient at 630 nm, which is the characteristic absorption band of iron(V)-oxo species. The natural decay of iron(V)-oxo species is relatively rapid at 0 °C (half-time of ~500 s, shown with black circles in Fig. 1a inset), but at −40 °C, the decay rate is in agreement with what has been published earlier ($t_{1/2}$ of around 2000 s).[11] After complete generation of **1**, we confirmed with ^1H NMR (Fig. S2, ESI†) that no excess m-CPBA exists in the solution before we add substrate.

The C-H bond activation of alkanes by **1** was then performed with substrates having C-H bond dissociation energies (BDEs) from 84.5 kcal mol^{-1} (cumene) to 99.3 kcal mol^{-1} (cyclohexane). Upon addition of ethylbenzene to a solution of **1**, the intermediate was converted to a new species (**2**) with isosbestic points at 415, 511, 564, and 715 nm (Fig. 1a). First-order rate constants, determined by the pseudo-first-order fitting of the kinetic data for the decay of **1** (Fig. 1a, inset), increased linearly with the increase of the ethylbenzene concentration (Fig. S3, ESI†), giving us a second-order rate constant of 4.5 x 10^{-1} M^{-1} s^{-1} at 0 °C. Noteworthy is that these reaction rates are at least 10-fold faster than the natural decay (Fig. 1a inset and Fig. S3, ESI†). A kinetic isotope effect (KIE) value of 11(1) was obtained in the ethylbenzene

oxidation by **1** (Fig. S3, ESI†). Similarly, second-order rate constants of **1** were determined in the oxidation of other substrates, showing a linear correlation between the reaction rates and the C-H BDEs of substrates (Fig. 1b and Fig. S4, ESI†). These results, such as a large KIE value and a good correlation between reaction rates and BDEs of substrates, demonstrate that a H-atom abstraction from the C-H bonds of substrates by **1** is the r.d.s. (Scheme 1B, pathway a).[6-8,14]

Product analysis of the reaction solution of the ethylbenzene oxidation by **1** revealed the formation of 1-phenylethanol (38 ± 4%) and styrene (12 ± 4%), and no formation of acetophenone was observed under Ar atmosphere.[8,14] When the ethylbenzene oxidation was performed with **1** in the presence of $H_2^{18}O$, the 1-phenylethanol product contained 50% of ^{18}O under Ar atmosphere (of maximum 60%, see Fig. S1). This result indicates that the source of oxygen in the hydroxylated product was the iron(V)-oxo species through oxygen exchange with water.[15] In contrast, when the ethylbenzene oxidation by **1** was carried out in the presence of air, the products formed were 1-phenylethanol (40 ± 4%), acetophenone (80 ± 8%), and styrene (7 ± 3%). Around 15% of 1-phenylethanol contained ^{18}O if the reaction was done in presence of $H_2^{18}O$ (Fig. S5, ESI†), demonstrating that O_2 might react with the substrate radical during the reaction. To support this conclusion, we carried out the hydroxylation of cyclohexane by **1** in the presence of CCl_3Br under Ar atmosphere. We observed the formation of bromocyclohexane as the sole product, showing that the formed substrate radical indeed can react with molecules outside the FeO-substrate cage.[4a]

We also characterized the decayed product **2** formed in the ethylbenzene oxidation by **1** (see Fig. 1a, blue line). ESI-MS of **2** exhibits a prominent peak at m/z 581.1 (Fig. S6, ESI†), whose mass and isotope distribution patterns correspond to $[Fe(IV)(TAML)(m-CBA)]^−$. The X-band EPR spectrum of **2** was silent, suggesting the oxidation state of +4 for the Fe ion in **2** (Fig. S6, ESI†). While the UV-spectrum is identical to that of the natural decay of **1**, the reaction rate is at least 10 times faster than the natural decay, and the majority of the Fe(IV) product should be from the C-H activation reaction. Further, addition of ferrocene (Fc) to the resulting solution caused the regeneration of $[Fe(III)(TAML)]^−$ and the formation of ~85% Fc$^+$ (Fig. S7, ESI†), supporting that **2** is an iron(IV) species. Based on these results, we propose that a monomeric Fe(IV) species, not a dimeric μ-oxo-$[Fe(IV)(TAML)]_2$ species (Fig. S8, ESI†), was formed in the C-H bond activation of hydrocarbons by **1**.

Then, how is the one electron-reduced Fe(IV) complex **2** formed in the alkane hydroxylation by **1**? This observation is contrary to the oxygen rebound mechanism; the hydroxylation of alkanes by Fe(V)-oxo species should afford Fe(III) species as a 2e$^−$ reduced product in the oxygen rebound mechanism.[4] Thus, the formation of the Fe(IV) complex **2** suggests that dissociation of the substrate radical (Scheme 1B, pathway c) is more favourable than the oxygen rebound process (Scheme 1B, pathway b), as we have shown in nonheme Fe(IV)-oxo, Mn(IV)-oxo, and Cr(IV)-oxo complexes.[7b,8] The reaction could then continue with a second Fe(V)O molecule reacting with the substrate radical, producing the observed substrate products (Scheme 1B, step d). The interference of O_2 and CCl_3Br in the experiments above supports this conclusion, as it shows the possibility of a third molecule reacting with the substrate radical. However, since we could not rule out a possibility that the Fe(IV) formation results from

comproportionation of **1** and Fe(III) species, we carried out a control reaction by reacting equal amounts of **1** and [Fe(III)(TAML)]⁻. In this reaction, the comproportionation reaction between **1** and [Fe(III)(TAML)]⁻ occurred rapidly;[13,14] however, the product formed was a μ-oxo-[Fe(IV)(TAML)]₂ (Fig. S8, ESI†) and this dimer product was different from the Fe(IV) complex formed in the hydroxylation of alkanes by **1**. Based on the results of product analysis, we propose that after Fe(IV)-OH and alkyl radical species are formed in the first step of the C–H bond activation by **1**, the dissociation process (Scheme 1B, pathway c) is a preferred pathway to the oxygen rebound process (Scheme 1B, pathway b). This hypothesis is supported by density functional theory (DFT) calculations (*vide infra*).

DFT calculations were performed at B3LYP/LACV3P*⁺//LACVP level with acetonitrile as solvent implemented through the CPCM model and Gaussian 09.[16] The lowest energy solution to the reactant structure produced a doublet [Fe(IV)(O)(TAML•⁺)]⁻ structure rather than [Fe(V)(O)(TAML)]⁻. Although no experimental support exists for this, earlier theoretical studies do report of such an electronic configuration.[17,18] Our investigation finds that this is a highly sensitive feature depending on the quality of the optimized geometry, which could be controlled by a proper choice of basis set (see ESI† for DFT methods). Since the main scope of these calculations is in the next step, where the potential initial ligand radical is of no consequence and the geometry is insensitive to different methods (*vide infra*), we merely note that different structures can be obtained for **1** depending on the methodology without affecting the next step of the reaction.

The C–H activation reaction by **1** was calculated using cyclohexane as a model substrate. The reaction in the $S = 1/2$ spin state is calculated to go through an energy barrier of 13.6 kcal/mol. Although the $S = 3/2$ state is only marginally higher in energy at the reactant state (0.8 kcal/mol), the barrier itself lies higher (18.9 kcal/mol) and is therefore ruled out at this stage. As the C–H activation involves an electron transfer as well as a proton transfer, the resulting intermediate is [Fe(IV)(OH)(TAML)]⁻, regardless whether the reactant structure is [Fe(V)(O)(TAML)]⁻ or [Fe(IV)(O)(TAML•⁺)]⁻. The obtained geometry here is insensitive to the basis set used (see ESI†, DFT methods section). At this point, there are four possible pathways to explore,[7b,8] such as 1) a rebound reaction takes place to give a hydroxylating product, 2) another H-atom is abstracted from the substrate to desaturate the substrate, 3) the spin state changes and the reaction continues on the $S = 3/2$ spin state, and 4) the substrate radical dissociates to react with another [Fe(V)(O)(TAML)]⁻. These options except the spin-state change possibility are depicted in Fig. 2. The first option (i.e., the rebound reaction) leads to a barrier of 4.7 kcal/mol relative to [Fe(IV)(OH)(TAML)]⁻, while the second option (i.e., desaturation) has a barrier of 7.6 kcal/mol. The third option requires the substrate radical to spin-flip, as the Fe(IV)(OH) moiety itself is already in its energetically lowest state. This leads to an $S = 3/2$ spin state, which is energetically degenerate (as expected) to $S = 1/2$. However, we have argued in a previous study[8b] that a spin flip of an organic radical, while can be fast, is still not fast enough to compete with energy barriers under 5 kcal/mol. The fourth option listed above, which is the dissociation process, requires only a dissociation energy of 1.6 kcal/mol; hence, we propose that dissociation occurs in the current compound as well, as supported by experiments (*vide supra*). The generality of the calculations are ensured by the strong C–H bond
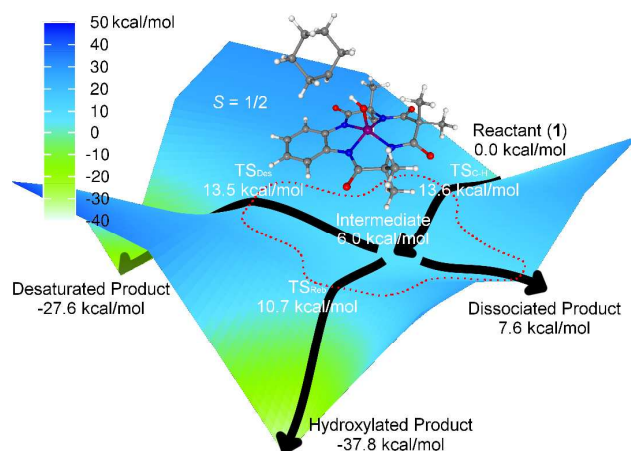

Fig. 2. Potential energy surface for the C–H activation reaction of cyclohexane by **1** in the $S = 1/2$ state. The initial rate-limiting C–H activation step occurs through a barrier of 13.6 kcal/mol to form an $Fe^{IV}OH$ intermediate. The so-formed substrate radial has now a multiple choice of pathways for the next step of the reaction (see text), and it is found that a simple dissociation is the energetically most favourable path to escape the cage (red dotted lines).

in cyclohexane; the feasibility shown for the C–H activation would presumably make the reaction feasible for weaker C–H bonds as well. Moreover, the relatively strong O–C bond in any rebound cyclohexanol product would lead to a larger driving force of the second part of the reaction than other weaker O–C bonds. Hence, for weaker O–C bonds, the rebound barrier is presumed to be lower by Bell-Evans-Polanyi principle,[19] making dissociation even more likely and these calculations should therefore be applicable to a range of other substrates as well.

In summary, we have provided experimental and theoretical evidence that the hydroxylation of alkanes by a mononuclear nonheme iron(V)-oxo complex occurs via a rate-determining H-atom abstraction, followed by an oxygen non-rebound process.

Notes and references

ᵃ Department of Chemistry and Nano Science, Ewha Womans University, Seoul 120-750, Korea. E-mail: wwnam@ewha.ac.kr.

1 (*a*) P. R. Ortiz de Montellano, *Cytochrome P450: Structure, Mechanism, and Biochemistry*, 3rd ed., Kluwer Academic/Plenum Publishers, New York. 2005; (*b*) S. Shaik, H. Hirao and D. Kumar, *Acc. Chem. Res.*, 2007, **40**, 532; (*c*) M. T. Green, *Curr. Opin. Chem. Biol.*, 2009, **13**, 84; (*d*) J. Rittle and M. T. Green, *Science*, 2010, **330**, 933; (*e*) M. C. White, *Science*, 2012, **335**, 807.
2 (*a*) C. Krebs, D. G. Fujimori, C. T. Walsh and J. M. Bollinger Jr., *Acc. Chem. Res.*, 2007, **40**, 484; (*b*) W. Nam, *Acc. Chem. Res.*, 2007, **40**, 522; (*c*) J. Hohenberger, K. Ray and K. Meyer, *Nat. Commun.*, 2012, **3**, 1; (*d*) S. P. de Visser, J.-U. Rohde, Y.-M. Lee, J. Cho and W. Nam, *Coord. Chem. Rev.*, 2013, **257**, 381; (*e*) A. R. McDonald and L. Que, Jr., *Coord. Chem. Rev.*, 2013, **257**, 414.

ChemComm Accepted Manuscript

3   (a) C.-M. Che, V. K.-Y. Lo, C.-Y. Zhou and J.-S. Huang, *Chem. Soc. Rev.*, 2011, **40**, 1950; (b) M. Costas, *Coord. Chem. Rev.*, 2011, **255**, 2912.

4   (a) J. T. Groves, *J. Chem. Educ.,* 1985, **62**, 928; (b) J. T. Groves, *Proc. Natl. Acad. Sci. U. S. A.,* 2003, **100**, 3569; (c) J. T. Groves, *J. Inorg. Biochem.,* 2006, **100**, 434.

5   (a) J. C. Price, E. W. Barr, B. Tirupati, J. M. Bollinger Jr. and C. Krebs, *Biochemistry*, 2003, **42**, 7497; (b) J.-U. Rohde, J.-H. In, M. H. Lim, W. W. Brennessel, M. R. Bukowski, A. Stubna, E. Münck, W. Nam and L. Que Jr., *Science*, 2003, **299**, 1037.

6   (a) J. Kaizer, E. J. Klinker, N. Y. Oh, J.-U. Rohde, W. J. Song, A. Stubna, J. Kim, E. Münck, W. Nam and L. Que Jr., *J. Am. Chem. Soc.,* 2004, **126**, 472; (b) C. V. Sastri, J. Lee, K. Oh, Y. J. Lee, J. Lee, T. A. Jackson, K. Ray, H. Hirao, W. Shin, J. A. Halfen, J. Kim, L. Que Jr., S. Shaik and W. Nam, *Proc. Nat. Acad. Sci. U.S.A.,* 2007, **104**, 19181.

7   (a) A. Company, I. Prat, J. R. Frisch, R. Mas-Ballesté, M. Güell, G. Juhász, X. Ribas, E. Münck, J. M. Luis, L. Que Jr., M. Costas, *Chem.-Eur. J.*, 2011, **17**, 1622; (b) K.-B. Cho, X. Wu, Y.-M. Lee, Y. H. Kwon, S. Shaik and W. Nam, *J. Am. Chem. Soc.*, 2012, **134**, 20222.

8   (a) X. Wu, M. S. Seo, K. M. Davis, Y.-M. Lee, J. Chen, K.-B. Cho, Y. N. Pushkar and W. Nam, *J. Am. Chem. Soc.,* 2011, **133**, 20088; (b) K.-B. Cho, S. Shaik and W. Nam, *J. Phys. Chem. Lett.,* 2012, **3**, 2851; (c) K.-B. Cho, H. Kang, J. Woo, Y. J. Park, M. S. Seo, J. Cho and W. Nam, *Inorg. Chem.*, 2014, **53**, 645.

9   (a) E. G. Kovaleva, M. B. Neibergall, S. Chakrabarty and J. D. Lipscomb, *Acc. Chem. Res.,* 2007, **40**, 475; (b) T. D. B. Timothy and S. Ramaswamy, *Curr. Opin. Chem. Biol.,* 2008, **12**, 134.

10 (a) S. H. Lee, J. H. Han, H. Kwak, S. J. Lee, E. Y. Lee, H. J. Kim, J. H. Lee, C. Bae, S. N. Lee, Y. Kim and C. Kim, *Chem.–Eur. J.*, 2007, **13**, 9393; (b) J. Yoon, S. A. Wilson, Y. K. Jang, M. S. Seo, K. Neru, B. Hedman, K. O. Hodgson, E. Bill, E. I. Solomon and W. Nam, *Angew. Chem., Int. Ed.*, 2009, **48**, 1257; (c) I. Prat, J. S. Mathieson, M. Güell, X. Ribas, J. M. Luis, L. Cronin and M. Costas, *Nat. Chem.*, 2011, **3**, 788; (d) E. P. Talsi and K. P. Bryliakov, *Coor. Chem. Rev.*, 2012, **256**, 1418; (e) O. Y. Lyakin, R. V. Ottenbacher, K. P. Bryliakov and E. P. Talsi, *Top. Catal.*, 2013, **56**, 939; (f) C.-W. Tse, T. W.-S. Chow, Z. Guo, H. K. Lee, J.-S. Huang and C.-M. Che, *Angew. Chem., Int. Ed.*, 2013, **52**, 1.

11 F. T. de Oliveira, A. Chanda, D. Banerjee, X. Shan, S. Mondal, L. Que Jr., E. L. Bominaar, E. Münck and T. J. Collins, *Science*, 2007, **315**, 835.

12 K. M. Van Heuvelen, A. T. Fiedler, X. Shan, R. D. De Hont, K. K. Meier, E. L. Bominaar, E. Münck and L. Que Jr., *Proc. Natl. Acad. Sci. U. S. A.,* 2012, **109**, 11933.

13 S. Kundu, J. V. K. Thompson, A. D. Ryabov and T. J. Collins, *J. Am. Chem. Soc.*, 2011, **133**, 18546.

14 M. Ghosh, K. K. Singh, C. Panda, A. Weitz, M. P. Hendrich, T. J. Collins, B. B. Dhar, S. S. Gupta, *J. Am. Chem. Soc.*, 2014, DOI:10.1021/ja412537m.

15 (a) J. Bernadou, A.-S. Fabiano, A. Robert and B. Meunier, *J. Am. Chem. Soc.*, 1994, **116**, 9375; (b) M. S. Seo, J.-H. In, S. O. Kim, N. Y. Oh, J. Hong, J. Kim, L. Que Jr. and W. Nam, *Angew. Chem., Int. Ed.*, 2004, **43**, 2417.

16 (a) A. D. Becke, *Phys. Rev. A,* 1988, **38**, 3098; (b) A. D. Becke, *J. Chem. Phys.,* 1993, **98**, 1372; (c) A. D. Becke, *J. Chem. Phys.,* 1993, **98**, 5648; (d) C. Lee, W. Yang and R. G. Parr, *Phys. Rev. B,* 1988, **37**, 785; (e) P. J. Hay and W. R. Wadt, *J. Chem. Phys.,* 1985, **82**, 299; (f) K. G. Dyall, *Theor. Chem. Acc.,* 2004, **112**, 403; (g) V. Barone and M. Cossi, *J. Phys. Chem., A*, 1998, **102**, 1995; (h) M. J. Frisch *et al. Gaussian 09, Revision B.01*, Gaussian Inc.: Wallingford CT, 2009. See ESI† reference S5 for full reference.

17 Calculations found a ligand radical on (TAML•+)Fe^{IV}OH systems: R.-Z. Liao, X.-C. Li and P. E. M. Siegbahn, *Eur. J. Inorg. Chem.*, 2014, **2014**, 728.

18 [Fe(IV)(O)(TAML•+)]$^−$ was found in the high-spin state and was explored as a possibility in the low-spin state as well; see ESI† in reference 11.

19 (a) P. Bell, *Proc. R. Soc. London, Ser. A*, 1936, **154**, 414; (b) M. G. Evans and M. Polanyi, *Trans. Faraday Soc.*, 1935, **31**, 875.

ChemComm Accepted Manuscript

Table of Contents Graphic
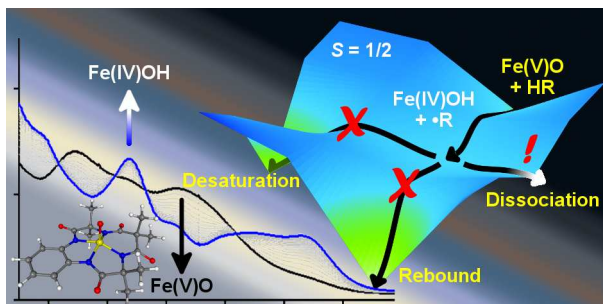
Synopsis: The alkane hydroxylation by a mononuclear nonheme iron(V)-oxo complex occurs via a hydrogen-atom abstraction/oxygen non-rebound mechanism.

ChemComm Accepted Manuscript